Electronic Supplementary Material (ESI) for ChemComm.

Supplementary Information

Spontaneous chirality through mixing achiral components: A twist-bend nematic phase driven by hydrogen-bonding between unlike components

*Rebecca Walker[a], Damian Pociecha[c], Jordan P Abberley[a], Alfonso Martinez-Felipe[b] , Daniel A Paterson[a], Ewan Forsyth[a], Gaynor B Lawrence[a], Peter A Henderson[a], John M D Storey[a], Ewa Gorecka[c], and Corrie T Imrie[a, *]*

[a]Department of Chemistry, and [b]Chemical and Materials Engineering Group, School of Engineering, King's College, University of Aberdeen, Aberdeen, AB24 3UE, UK

[c]University of Warsaw, Department of Chemistry, ul. Zwirki i Wigury 101, 02-089 ˙ Warsaw, Poland

*Author for correspondence; email c.t.imrie@abdn.ac.uk

Table of Contents

Section A. Materials / General Methods / Instrumentation

Materials

All reagents and solvents were available commercially and purchased from Sigma Aldrich, Alfa Aesar or TCI Chemicals and used as received unless otherwise stated. Silica gel for column chromatography, grade 60 Å 40-63 micron, was purchased from Flurochem. Reactions were monitored using Thin Layer Chromatography (TLC) and an appropriate solvent system. Silica gel coated aluminium plates were purchased from Merck KGaA. Spots were visualised using UV light (254 nm).

Butyloxybenzoic (4OBA) and pentyloxybenzoic (5OBA) acid were purchased from Sigma Aldrich and purified by recrystallisation from ethanol (10 mL per g).

General Methods and Instrumentation

The proposed structures of all the final products were characterised using a combination of ^{1}H and ^{13}C NMR, and FT-IR spectroscopies. ^{1}H and ^{13}C NMR spectra were recorded on either a 400 MHz Varian Unity INOVA, or a 300 MHz Bruker Ultrashield NMR spectrometer. Infrared spectra were recorded on a Thermal Scientific Nicolet IR100 FT-IR spectrometer with an ATR diamond cell.

The purities of the final products were verified using C, H, N microanalysis performed by the Micro Analytical Laboratory in the School of Chemistry at the University of Manchester.

Section B. Synthetic protocols and characterisation

The synthetic route used to prepare 4-[(E)-2-(4-{[6-(4'-methoxy[1,1'-biphenyl]-4-yl)hexyl]oxy}phenyl)ethenyl]pyridine (1OB6OS) is shown in Scheme 1.

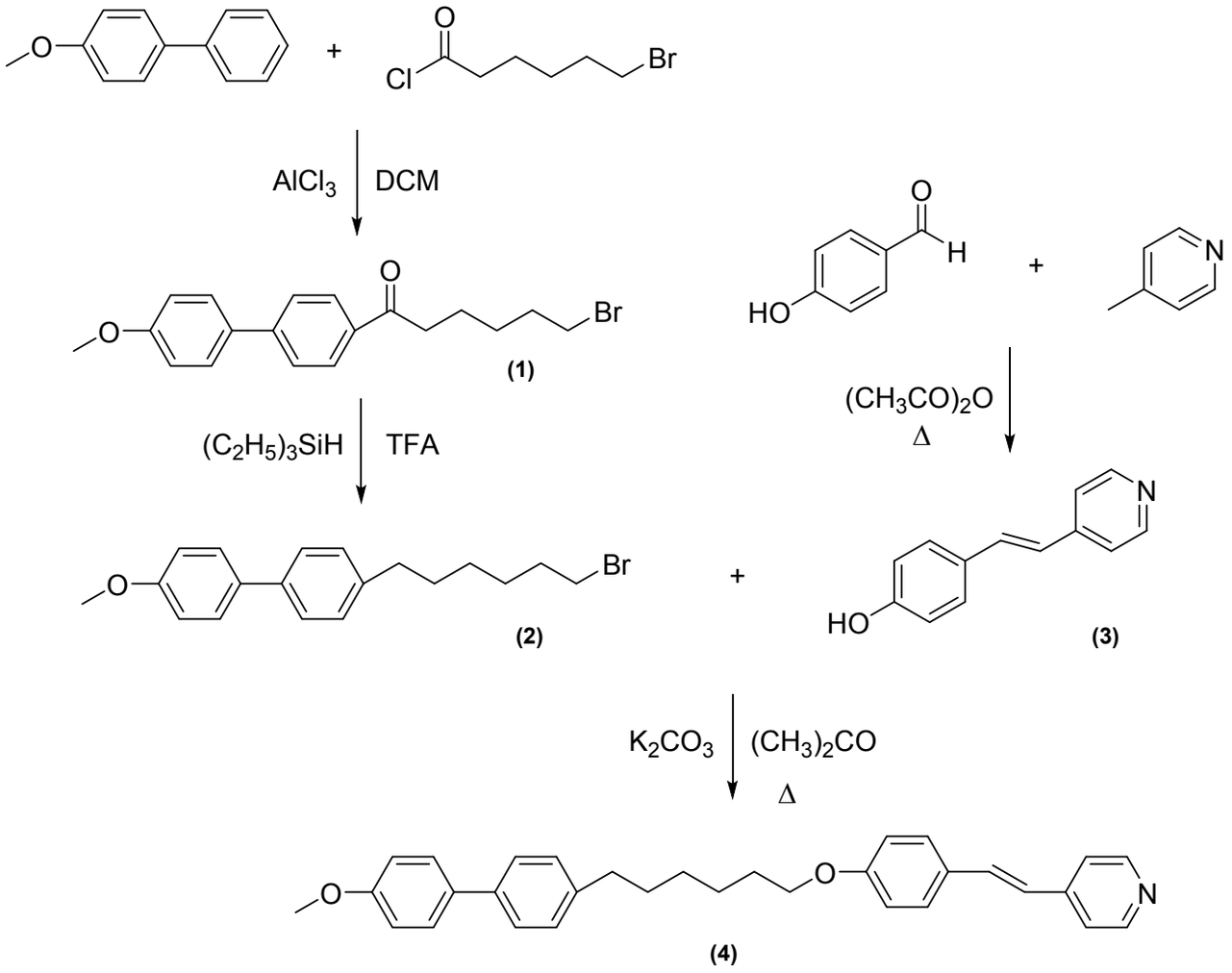

Scheme 1. Synthesis of 1OB6OS

*6-bromo-1-(4'-methoxy[1,1'-biphenyl]-4-yl)hexan-1-one (**1**)*

The synthesis of **1** followed the method described by Abberley et al [1]. Thus, a mixture of 4-methoxybiphenyl (3.174 g, 0.017 mol) and 6-bromohexanoyl chloride (4.2 g, 0.020 mol) dissolved in dichloromethane (25 mL) was added dropwise to a stirred suspension of aluminium (III) chloride (3.687 g, 0.027 mol) in dichloromethane (150 mL), cooled to 0 °C in an ice bath. The resulting mixture was allowed to warm to room temperature and stirred for 20 h. The mixture was then added to 100 g of crushed ice and 10 mL concentrated

hydrochloric acid before extraction using dichloromethane (2 x 50 mL). The organic fractions were combined, dried over anhydrous $MgSO_4$ and the solvent removed in vacuo. The crude product was recrystallised from ethanol to give the title compound as an off-white solid. Yield: 3.786 g, 61.6 %.

IR $\bar{\nu}$ cm^{-1}: 2944, 2870, 1677 (C=O ketone), 1598, 1496, 1254, 1180, 1034, 806. ^{1}H NMR (300 MHz, $CDCl_3$) δ ppm: 1.49 - 1.66 (m, 2 H. $ArCOCH_2CH_2\underline{CH_2}CH_2CH_2Br$), 1.82 (quin, J = 7.49 Hz, 2 H. $ArCOCH_2\underline{CH_2}CH_2CH_2CH_2Br$), 1.95 (quin, J = 7.11 Hz, 2 H. $ArCOCH_2CH_2CH_2\underline{CH_2}CH_2Br$), 3.03 (t, J = 7.25 Hz, 2 H. $ArCO\underline{CH_2}CH_2CH_2CH_2CH_2Br$), 3.46 (t, J = 6.78 Hz, 2 H. $ArCOCH_2CH_2CH_2CH_2\underline{CH_2}Br$), 3.89 (s, 3 H. $\underline{CH_3}OAr$-), 7.02 (d, J = 8.67 Hz, 2 H. Ar), 7.50 - 7.80 (m, 4 H. Ar), 8.03 (d, J = 8.48 Hz, 2 H. Ar). ^{13}C NMR (75 MHz, $CDCl_3$) δ ppm: 23.45, 27.92, 32.66, 33.62, 38.27, 55.38, 114.43, 126.64, 128.35, 128.65, 132.27, 135.09, 145.27, 159.93, 199.53.

*4-(6-bromohexyl)-4'-methoxy-1,1'- biphenyl (**2**)*

The synthesis of **2** followed the method described by Abberley et al [1]. Triethylsilane (6.7 mL, 0.0419 mol) was added dropwise to a mixture of 6-bromo-1-(4'-methoxy[1,1'-biphenyl]-4-yl)hexan-1-one (3.786 g, 0.0105 mol) and trifluoroacetic acid (6.5 mL, 0.0838 mol) in dichloromethane (20 mL), cooled to 0 °C in an ice bath. The resulting mixture was stirred for 16 h at room temperature before addition to water (75 mL) and dichloromethane (25 mL). The layers were separated and the aqueous layer washed with dichloromethane (2 x 50 mL). The organic fractions were combined and dried over anhydrous $MgSO_4$ before removal of the solvent in vacuo. The crude product was recrystallised from ethanol to give the title compound as a white solid. Yield: 1.511 g, 41.4 %.

IR $\bar{\nu}$ cm^{-1}: 2933, 2858, 1606 (para di-substituted benzene), 1498, 1464, 1282, 1182, 1037, 813, 641, 513. ^{1}H NMR (300 MHz, $CDCl_3$) δ ppm: 1.34 - 1.55 (m, 4 H. $Ar\text{-}CH_2CH_2\underline{CH_2}\underline{CH_2}CH_2CH_2\text{-}Br$), 1.69 (quin, J = 6.00 Hz, 2 H. $Ar\text{-}CH_2\underline{CH_2}CH_2CH_2CH_2CH_2\text{-}Br$), 1.89 (quin, J = 7.06 Hz, 2 H. $Ar\text{-}CH_2CH_2CH_2CH_2\underline{CH_2}CH_2\text{-}Br$), 2.61 - 2.72 (m, 2 H. $Ar\text{-}\underline{CH_2}CH_2CH_2CH_2CH_2CH_2\text{-}Br$), 3.43 (t, J = 6.78 Hz, 2 H. $Ar\text{-}CH_2CH_2CH_2CH_2CH_2\underline{CH_2}\text{-}Br$), 3.87 (s, 3 H. $\underline{CH_3}$-OAr), 6.99 (d, J = 8.85 Hz, 2 H. Ar), 7.24 (d, J = 8.29 Hz, 2 H. Ar), 7.46 - 7.58 (m, 4 H. Ar). ^{13}C NMR (75 MHz, $CDCl_3$) δ ppm: 28.07, 28.44, 31.27, 32.77, 33.97, 35.43, 55.36, 114.19, 126.63, 127.98, 128.80, 133.72, 138.30, 141.06, 158.98.

4-[(E)-2-(pyridin-4-yl)ethenyl]phenol (3)

A stirred mixture of 4-methylpyridine (10 ml, 0.103 mol) and 4-hydroxybenzaldehyde (15.270 g, 0.125 mol) in acetic anhydride (21.5 ml, 0.226 mol) was heated under reflux for 23 hr. After cooling to room temperature, the mixture was poured into ice water (600 ml) and

stirred for 1 h. The resulting precipitate was collected using vacuum filtration and refluxed in alcoholic potassium hydroxide (0.75 N) for 2 h. Acetic acid (20 ml) was added to precipitate the crude product, which was recrystallised from ethanol to give the title compound as a dark yellow solid. Yield: 6.852 g, 33.7 %.

IR $\bar{\nu}$ cm^{-1}: 3250-2000 (broad, OH), 1636 (C=C), 1581, 1512, 1250, 1192, 973, 829, 547. ^{1}H NMR (300 MHz, DMSO-d_6) δ ppm 6.80 (d, *J* = 8.67 Hz, 2 H), 7.01 (d, *J* = 16.58 Hz, 1 H. Ar-CHCH-Ar), 7.39 - 7.53 (m, 5 H. Ar-CHCH-Ar, Ar), 8.46 - 8.54 (m, 2 H. Ar, adj. to N), 9.77 (s, 1 H. OH-Ar). ^{13}C NMR (75 MHz, $CDCl_3$) δ ppm: 115.64, 120.45, 122.43, 127.17, 128.63, 133.02, 144.76, 149.86, 158.18.

4-[(E)-2-(4-{[6-(4'-methoxy[1,1'-biphenyl]-4-yl)hexyl]oxy}phenyl)ethenyl]pyridine (4)

A stirred mixture of 4-hydroxystilbazole (0.791 g, 0.0040 mol), 4-(6-bromohexyl)-4'-methoxy-1,1'-biphenyl (1.384 g, 0.0040 mol) and potassium carbonate (1.211 g, 0.0086 mol) in acetone was heated under reflux at 65 °C for 96 h. After cooling to room temperature, the resulting precipitate removed by vacuum filtration and the filtrate removed in vacuo to yield a dark brown solid. The crude product was purified by first passing through silica, washing through with copious amounts of ethyl acetate and subsequent recrystallisation in a 2:1 mixture of ethanol and ethyl acetate to give the title compound as a golden solid. RF = 0.51 in 80:20 ethyl acetate & petroleum ether (40/60). Yield: 1.175 g, 63.4%.

Melting point: 133.61 °C. IR $\bar{\nu}$ cm^{-1}: 2914, 2849, 1671, 1605, 1588, 1499, 1254, 1177, 1019, 972, 822, 545. ^{1}H NMR (300 MHz, $CDCl_3$) δ ppm: 1.40 - 1.62 (m, 4 H. Ar-$CH_2CH_2CH_2CH_2CH_2CH_2$O-Ar), 1.65 - 1.77 (m, 2 H. Ar-$CH_2CH_2CH_2CH_2CH_2CH_2$O-Ar), 1.78 - 1.91 (m, 2 H. Ar-$CH_2CH_2CH_2CH_2CH_2CH_2$O-Ar), 2.68 (t, *J* = 7.63 Hz, 2 H. Ar-$CH_2CH_2CH_2CH_2CH_2CH_2$O-Ar), 3.86 (s, 3 H. CH_3O-Ar), 4.01 (t, *J* = 6.50 Hz, 2 H. Ar-$CH_2CH_2CH_2CH_2CH_2CH_2$O-Ar), 6.85 - 6.95 (m, 3 H. Ar, OAr-CHCH-Ar), 6.98 (d, *J* = 8.85 Hz, 2 H. Ar), 7.22 - 7.33 (m, 3 H. Ar, OAr-CHCH-Ar), 7.38 (d, *J* = 6.22 Hz, 2 H. Ar), 7.49 (dd, *J*=8.38, 1.60 Hz, 4 H. Ar), 7.51 - 7.57 (m, 2 H. Ar), 8.57 (d, *J* = 5.84 Hz, 2 H. Ar (adj. to N)) ^{13}C NMR (75 MHz, $CDCl_3$) δ ppm: 25.90, 28.95, 29.12, 31.38, 35.43, 55.34, 68.00, 114.15, 114.83, 120.65, 123.55, 126.60, 127.98, 128.40, 128.68, 128.81, 132.81, 133.68, 138.22, 141.16, 145.05, 150.09, 158.92, 159.75. Elemental Analysis: Calculated for $C_{32}H_{33}NO_2$: C 82.90 %, H 7.17 %, N 3.02 %, Found: C 82.61 %, H 7.15 %, N 2.99 %.

Section C. Physical characterisation

Thermal Analysis

The thermal behaviour of the binary mixtures was investigated by differential scanning calorimetry (DSC) using a Mettler Toledo DSC822e differential scanning calorimeter equipped with a TSO 801RO sample robot and calibrated using indium and zinc standards. The heating profile in all cases was heat, cool and reheat at 10 °C min^{-1} with a 3-minute isotherm between heating and cooling segments and under an inert atmosphere of nitrogen. Thermal data were normally extracted from the second heating trace.

Optical Properties

Phase characterisation was performed using polarised light microscopy using an Olympus BH2 polarising light microscope equipped with a Linkam TMS 92 hot stage (Aberdeen) and Zeiss Imager A2m polarizing microscope equipped with Linkam heating stage (Warsaw). Glass cells were provided by WAT having 1.6 micron thickness, ITO and 60 polymer aligning layer were used.

X-Ray Diffraction

The small angle X-ray diffraction (SAXRD) patterns for powder samples were obtained with a Bruker Nanostar system using CuKα radiation and patterns were collected with an area detector VANTEC2000. The temperature of the sample was controlled with precision of ± 0.1 K. Samples were prepared either in thin-walled glass capillaries or as droplets on heated surface. Wide angle diffractograms (WAXS) were obtained with a Bruker D8 GADDS system (CuKα line, Goebel mirror, point beam collimator, Vantec2000 area detector).

Fourier Transform Infrared Spectroscopy, FT-IR

Temperature dependent infrared spectra were recorded on a Nicolet Nexus attached to a Continuum FT-IR microscope equipped with a Linkam FT-IR 600 heating stage and a TMS 93 control unit. Samples were ground and pressed into a 3 mm KBr disc for analysis. The materials were melted into the isotropic phase in order to remove any thermal history, and data were collected on cooling to room temperature in steps of 10 °C.

Section D. Computer modelling

In order to estimate the geometric parameters, electronic properties and hydrogen bond dissociation energies, quantum mechanical density functional theory (DFT) calculations were used [2]. Geometric optimisation was performed on the MeOB6OS:4OBA complex using Gaussian G09W with the spacer in the all-*trans* conformation at the B3LYP/6-31G(d) level of theory. It has been reported, however, that the all-*trans* state of the hexyloxy spacer is not the ground state and instead a *gauche* defect about the O-C-C-C dihedral is more stable than the *trans* form [3]. Geometric optimisation was therefore also performed at the B3LYP/6-31G(d) level of theory with the spacer containing this gauche state. However the difference in energy between these two states was found to be very small (~1 kJ/mol) and similar to those reported elsewhere for other methylene-ether linked dimers [1, 3-4]. We also note that the energy profiles are likely to be somewhat different in a liquid crystal environment in which the more elongated conformers of the dimer will be favoured [3]. Thus, when calculating the hydrogen bond dissociation energy, the all-*trans* conformation was selected. In order to increase the accuracy in calculating the hydrogen bond dissociation energies by minimising basis set superposition errors and accounting for dispersion forces, geometrical counterpoise (gCP) and D3 corrections were made to the self-consistent field (SCF) energy post-optimisation of both complexes using the online gCP-D3 correction facility developed by Grimme and coworkers [5]. To calculate the SCF energies of the separated complexes, each hydrogen bond of the optimised complexes was extended to a distance of 5 Å, and a single point energy calculation performed (Table S1). For visualisation of space filling models QuteMol was used [6], and for visualisation of electrostatic potential isosurfaces, ball-and-stick models and dipole moments, GaussView 5 was used [7].

Table S1. Hydrogen bond strength parameters calculated from density functional theory geometry optimisation at the B3LYP/6-31G(d) level of theory, with gCP-D3 corrections applied post-optimisation to determine the hydrogen bond dissociation energy.

Complex	Average hydrogen atom to hydrogen bond acceptor length (Å) in optimised structure	Hydrogen bond dissociation energy ($kJ.mol^{-1}$)
4OBA Closed dimer	1.672	86.50
MeOB6OS:4OBA	1.759	61.41

Section E. Additional data

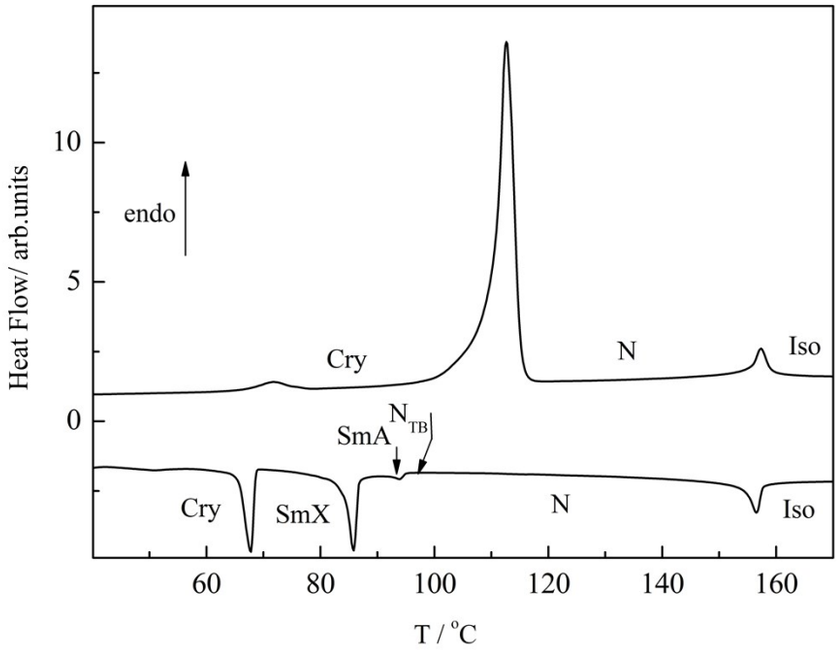

Figure S1. First heating and subsequent cooling DSC scans for the *10B6OS:5OBA* complex.

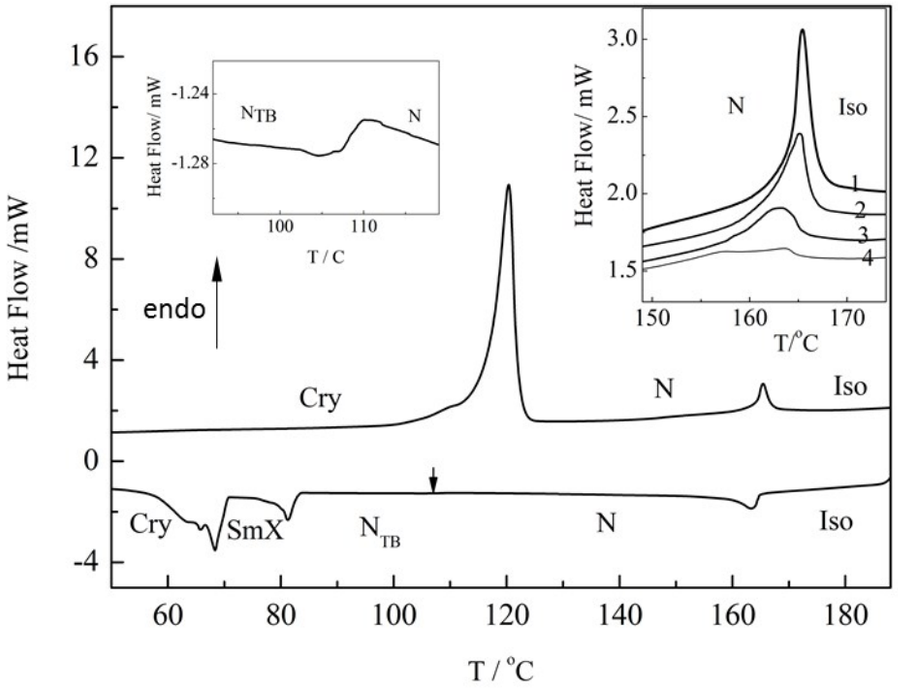

Figure S2. First heating and subsequent cooling DSC scans for the*10B6OS:4OBA* mixture. In the left inset enlarged region of N-N_{TB} phase transition. In the right inset enlarged region of nematic-isotropic phase transition, in which several consecutive heating scans are shown (*1- 4*). The increasing two-phase region indicates that the stability of the complex decreases upon entering the isotropic phase in sequential runs.

References

[1] J. P. Abberley, S. M. Jansze, R. Walker, D. A. Paterson, P. A. Henderson, A. T. M. Marcelis, J. M. D. Storey, C. T. Imrie, *Liq. Cryst.* 2017, *44*, 68-83.

[2] M. J. Frisch, e. al., *Gaussian 09 (Revision B.01)*, Gaussian Inc., Wallingford CT, 2010.

[3] D. A. Paterson, M. Gao, Y. K. Kim, A. Jamali, K. L. Finley, B. Robles-Hernandez, S. Diez-Berart, J. Salud, M. R. de la Fuente, B. A. Timimi, H. Zimmermann, C. Greco, A. Ferrarini, J. M. D. Storey, D. O. Lopez, O. D. Lavrentovich, G. R. Luckhurst, C. T. Imrie, *Soft Matter* 2016, *12*, 6827-6840.

[4] D. A. Paterson, J. P. Abberley, W. T. Harrison, J. M. Storey, C. T. Imrie, *Liq. Cryst.* 2017, *44*, 127-146.

[5] H. Kruse, L. Goerigk, S. Grimme, *J. Org. Chem.* 2012, *77*, 10824-10834.

[6] M. Tarini, P. Cignoni, C. Montani, *IEEE Trans. Visualization and Computer Graphics* 2006, *12*, 1237-1244.

[7] R. Dennington, T. Keith, J. Millam, Gauss view, version 5. Semichem Inc, Shawnee Mission, KS, 2009.